

Measuring Spinous Process Angle on Ultrasound Spine Images using the GVF Segmentation Method

Honeyge Zeng¹
School of Information Science
and Technology
ShanghaiTech University
Shanghai, China
zenghy@shanghaitech.edu.cn

Rui Zheng^{1*}
School of Information Science
and Technology
ShanghaiTech University
Shanghai, China
zhengrui@shanghaitech.edu.cn

Lawrence H Le²
Department of Radiology and
Diagnostic Imaging
University of Alberta
Edmonton, Canada
lel@ualberta.ca

Dean Ta³
Department of Electronic
Engineering
Fudan University
Shanghai, China
tda@fudan.edu.cn

Abstract—Spinous process angle (SPA) is an important parameter to evaluate the severity of scoliosis. However, the spinous process cannot be accurately automatic located due to the interference of the muscle layer. The objectives of this study are to apply gradient vector flow (GVF) snake model to segment spinous process (SP) on US transverse vertebral images and to illustrate and measure SPA on US coronal spine images. The snake method could detect SP tip position reliably in this study. Ten spinous process curves were identified on both radiographs and US images. The mean absolute difference (MAD) of SPAs obtained from the two modalities was $2.5 \pm 1.9^\circ$. It demonstrates the SPA measured from US images via GVF snake model is comparable with the results from the conventional radiographs.

Keywords—GVF Snake Model, US image segmentation, US spine imaging, Spinous Process Angle, Scoliosis.

I. INTRODUCTION

Adolescent idiopathic scoliosis (AIS) is a three-dimensional (3D) deformity of the spine characterized by lateral curvature and vertebral rotation. It occurs in approximately 5.14% of adolescents in China, and 14 and 15-year-old girls shows the highest prevalence rates (13.81%) [1]. Radiography is conventionally used to detect and monitor scoliosis, but it can cause high dose of ionizing radiation to patients [2]. Ultrasound (US) imaging technique has become a promising diagnostic tool since it is radiation-free, cost-effective and portable comparing to radiography.

The US method has been applied for scoliosis assessment [3-6]. Chen et al demonstrated that the bony landmarks can be identified on US images for measuring spinal deformity [3]. The center of lamina (COL) method was proposed, and the lamina were used as reflectors to estimate the curvature of spine on US images [4]. The measurement difference between COL method and radiography was $0.7 \pm 0.5^\circ$. Zheng et al verified the intra- and inter-rater reliability of the US method furthermore [5]. Standard error of measurement on both intra- and inter-rater measurements using US methods was less than 2.8° , and the correlation coefficient between the US and radiographic methods ranged between 0.78 and 0.84 among 3 raters. Jiang et al proposed a new fast 3-D US projection

This work was sponsored by Natural Science Foundation of Shanghai

imaging method to evaluate spine deformity [6]. Their measurement results showed a high correlation ($y = 0.984x$, $r = 0.954$) between the developed projection method and conventional rendering method. The method could also decrease the processing time and may help to provide fast 3-D ultrasound diagnosis of scoliosis in clinics.

The SPA is an important parameter measured from spinous process (SP) curve to evaluate the posterior deformity of spine, and it is defined as continuous curve to connect all the tips of identified SP [7]. Since spinous process, the apex of vertebra, is usually merged into muscle layer on US images, the SPA cannot be obtained on the US coronal images directly. The gradient vector flow (GVF) snake model is a commonly used segmentation method proposed by Xu and Prince in 1997 [8]. In contrast to conventional snake model, the GVF snake model can capture surfaces of irregular object such as concave boundary, and simultaneously extend effective range influenced by external force in homogeneous area. It has been widely applied in medical image segmentation [9-11]. For example, the breast cancer nuclei could be segmented on the cytological images by the snake method [9]; The liver contour was semi-automatically delineated on contrast-enhanced CT images using snake algorithm [10]; A robust snake could be initialized and converged to liver tumor contour of various size on noisy and complex US images [11].

In this study, the GVF snake model is implemented for segmentation of spinous process on 2D US transverse vertebral images. SP curve will be illustrated on the coronal image, and SPA will be measured according to the SP curve. The SPAs measured from our method and radiography will be compared to verify the robustness and accuracy of the method.

II. METHOD

A snake is a deformable curve which can move to target curve via minimizing the energy function, and the movement is under the influence of internal force and external force. Using the position of a snake defined by $\varphi(s) = [x(s), y(s)]$, $s \in [0, 1]$, the energy function can be written as

$$E_{snake} = \int_0^1 \frac{1}{2} [\alpha |\varphi'(s)|^2 + \beta |\varphi''(s)|^2] + E_{ext}(\varphi(s)) ds \quad (1)$$

where, the first and second derivatives of $\varphi(s)$ indicate the internal force which maintains the basic shape of curve during deformation. α and β are weighting parameters that control the internal force [12]. The external force E_{ext} is derived from image intensity to move the snake to the region of interest (ROI) which is muscle/SP interface in this study.

The GVF snake model defines gradient vector flow field as external force. Given the vector field denoted as $v(x, y) = [u(x, y), v(x, y)]$, the energy function in the field can be expressed as [8]

$$E = \iint \mu (u_x^2 + u_y^2 + v_x^2 + v_y^2) + |\nabla f|^2 |v - \nabla f|^2 dx dy \quad (2)$$

where μ is the regularization parameter balancing the first term and the second term, and ∇f is the gradient of image data. By iteration, the GVF was approximate to the gradient when the gradient was large, and could yield a smooth field in homogeneous regions.

The process of the GVF snake model could be divided into three steps: 1) determining initial curve, 2) calculating GVF and 3) moving the curve to target. Some image processing methods were subsequently applied to identify SP position on target curve, and then all transverse images were reconstructed to obtain coronal US image for SPA measurement.

A. Determine initial curve

Figure 1 shows the procedure of determining the initial curve for the iteration. The initial curve was set to a proxy Sinc-shaped curve in the blank area between lamina and SP as illustrated in Figure 1a, since the contour line of vertebra is approximate to a Sinc curve on US transverse images. Lamina is located in the middle region of the transverse image with high brightness, therefore it can be straightforwardly detected using image processing methods.

To identify the lamina, the muscle layer was removed (Figure 1b) according to its high intensity and the location on the top of US transverse images. The Otsu's method [13] was used to maximize the distinction between ribs, lamina and background, and a binary image was produced with reserving ribs and lamina area (Figure 1c).

The fast-parallel thinning algorithm [14] was then applied to extract skeleton from the binary image, and the endpoints of lamina skeleton were detected. After extracting lamina and ribs as skeleton, the image was divided into two parts from the middle blank area to left and right sides, and the endpoints was defined as the pixels on the skeleton nearest to the middle line in each part (Figure 1d). The distance between two endpoints was set as the criteria to determine lamina position. The distance larger than the assigned threshold indicated that endpoints were located on ribs, and this image should be skipped. The green line connected two endpoints as shown on Figure 1e were set as bottom of initial curve. Theoretically the top of initial curve should be embedded in the muscle layer on US image. Therefore, the top position could be found along the vertical bisector of the bottom line.

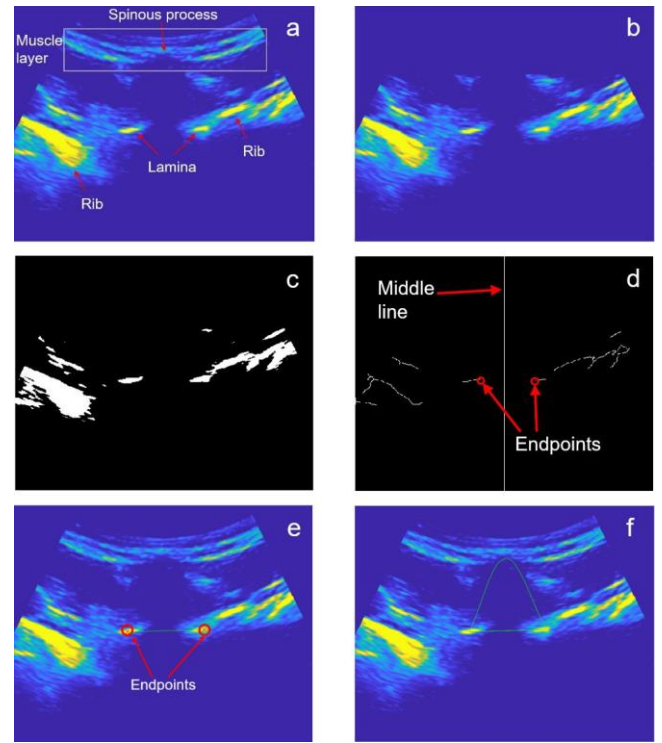


Figure 1. Determining initial curve for GVF snake model: (a) original US transverse images; (b) removing muscle layer; (c) Otsu's result; (d) skeleton result; endpoints was found on the skeleton nearest to the middle line in each part; (e) connecting endpoints as bottom line of initial curve; (f) the initial curve.

The two endpoints and top position were set as the zero points and peak of Sinc-shaped curve respectively, then the initial curve was derived from Sinc function as the green curve shown on Figure 1f.

B. Calculate GVF

The GVF was calculated via solving equation (2) iteratively. The parameter μ was set to 0.1, and the proper value of μ can preserve the GVF near the edge, simultaneously maintaining the GVF non-zero in the homogeneous area. The large number of iterations can obtain wider capture range, but the over-limited iterations number could jeopardize GVF result and cause non-convergence near the image edge. The maximum number of acceptable iterations was set as 200 in this study.

Before calculation, the gray image was converted to the binary image. The GVF of original gray US images were not able to completely converge onto muscle/SP interface and could attract curve into irrelevant muscle layer; while GVF of binary image could constrain the curve to ROI.

Figure 2b illustrates the GVF quiver vector map for part of a transverse vertebral image (Figure 2a). The GVF was almost equal to gradient at the contour of muscle layer for attracting and restraining curve to the muscle/SP interface, and it was nonzero in blank area to keep initial curve moving.

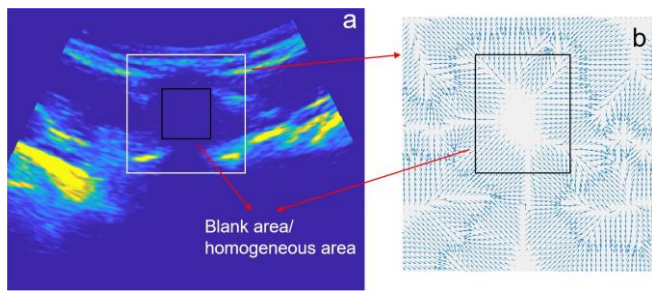


Figure 2. GVF quiver vector map for part of a transverse vertebral image (the area in white box).

C. Move curve to target

The curve movements were driven by minimizing the energy function of equation (1). During the test on 50 US images selected from different subjects and acquisition locations, the curve was always bound to target curve after 10-15 moves, therefore 15 movements were arranged for each image in this study. Since large number of iterations can make the moving step too big and cause the curve skip over the contour of muscle layer, all points on the curve were iterated for 10 times during each move.

Figure 3 illustrated the complete movements of initial curve under the influence of GVF. The green initial curve moved to red target curve, and the white curves displayed the moving tracks during the process. The target curve contained whole indentation of muscle layer around the SP, and would be used to extract the boundary of SP tip.

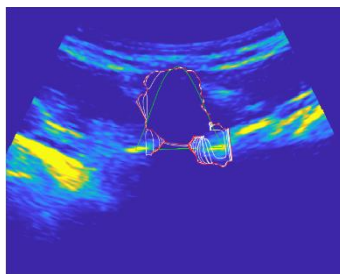


Figure 3. The curve movements.

D. Identify spinous process tip position

SP tip should be in the perpendicular bisector of the line segment connected two endpoints of lamina due to the anatomic structure of vertebra. The perpendicular bisector can be calculated from bottom of initial curve, and a 30-pixel wide region around perpendicular bisector was defined as ROI. The ROI was used as a mask on the target curve after iteration to find position range of SP tip, as illustrated on Figure 4a. The tip position range was illustrated as a small curve which was the top part of the target curve in the ROI. Since SP is the closest part of vertebra to the surface of human body, the top point of the small curve was denoted as the position of SP tip and its coordinate was obtained. Finally, the intensity of the pixel at the selected coordinates and its 8 neighbor pixels was assigned to 255 for visualizing on coronal image, and muscle layer was automatically removed for the further processing. The final segmentation result was shown on Figure 4b.

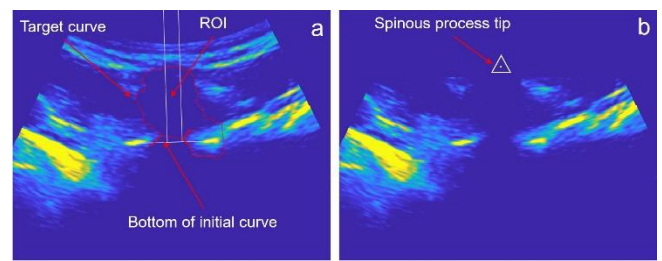


Figure 4. Processing on the GVF snake result: (a) ROI on US image; (b) the final segmentation result.

E. 3D reconstruction and SPA measurements

One US scan consisted of 1000-2000 transverse frames, and the GVF method was required to be applied on each frame to identify SP tip. The Voxel-Based Nearest Neighbor method (VNN) was used to reconstruct the 3D data volume and obtain coronal image of spine [15]. The 3D reconstruction result for one patient was as shown on Figure 5a, and the red dots in the middle was identified SP tips. The SP curve was determined on coronal image based on the marks from transverse images, and then the SPA can be measured manually.

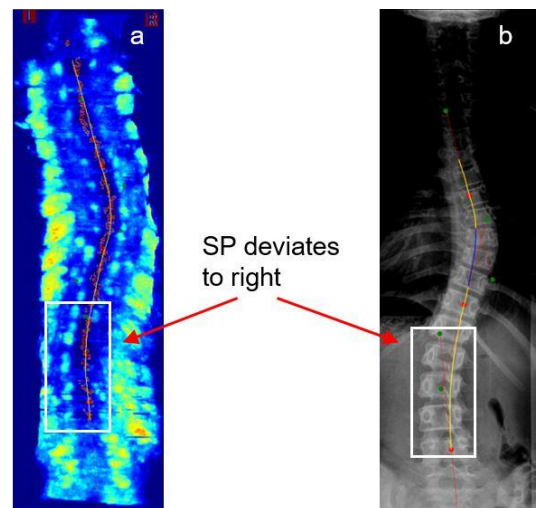


Figure 5. Spinous process curves illustrated on coronal images: (a) US image; (b) radiography.

F. SPA measurements and statistical analysis

Ten US scans from 10 adolescents (8 males and 2 females; mean age: 14.16 ± 2.44) were processed. They fulfilled the following inclusion criteria: 1) they had no prior surgical treatment; 2) they had a posterior-anterior standing radiograph and US scan within an hour; 3) the major curve was in the range of 10° to 45° .

The US coronal images and radiographs were measured using the same custom-developed software. An example of the measurement results was illustrated on Figure 5. The difference of SPA measurements from two methods were calculated. The correlation, mean absolute difference (MAD) and standard deviation (SD) between the results from two modalities were investigated.

III. RESULTS AND DISCUSSION

The SP curves could be determined on all 10 US coronal images acquired from patients, and 17 SPAs were measured. As an example indicated on Figure 5, the region of white box was lumbar area, and the SPA curves deviated to right on the US coronal image and radiography synchronously. The SPA curve measured from US image was qualitatively approximate to result from radiography.

The SPAs measured from radiographs and US images ranged 11-42° and 14-43°, and the mean values were 24.6±8.1° and 25.7±8.1° respectively. The mean absolute difference (MAD) of SPAs obtained from the two methods was 2.5±1.9°, which was less than the clinical acceptance error (5°) [16]. The correlation coefficient of SPAs measured from radiography and US images was 0.93, and the correlation curve was shown on Figure 6a. Figure 6b demonstrated that there is no apparent systemic error between the two method, and most of the measurement differences were within acceptable error.

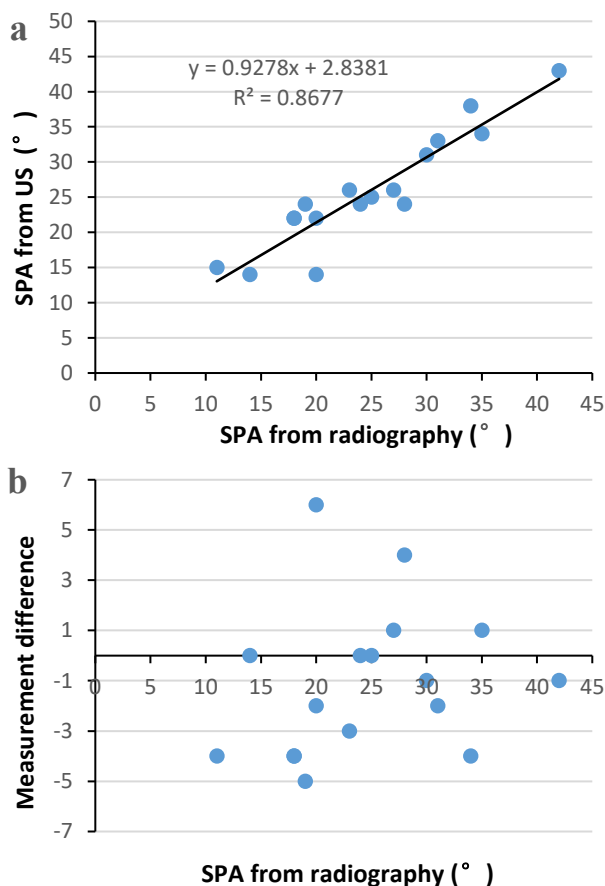


Figure 6. Comparison between radiographic and US measurements of SPAs: (a) the correlation, and (b) the measurement difference.

Even though the US method showed good feasibility and accuracy, locating lamina was still difficult and cause inaccurate results in some situation, and moreover lead to wrong SPA measurement. Especially when lamina was

unilaterally missing, one of the endpoints would be located on ribs, The SP position would be positioned on the vertical bisector of the rib and lamina, and deviated from the true position. The new methods will be furtherly proposed to distinguish the lamina type when unilateral missing case occurred, and under this circumstance, both endpoints will be located on lamina.

IV. CONCLUSION

The GVF snake model can be used to identify spinous process tip on US transverse images, and furthermore to illustrate the spinous process curve on US coronal images. The SPA can be measured from the US images, and the MAD of SPAs measured using our method and conventional radiography were less than clinical acceptance error. It indicates that the GVF snake model method is applicable for the SPA measurement on US images.

REFERENCES

- [1] H. Fan et al., 'Prevalence of Idiopathic Scoliosis in Chinese Schoolchildren', *SPINE*, vol. 41, pp. 259-264, Feb. 2016.
- [2] 'Breast cancer in women with scoliosis exposed to multiple diagnostic x rays', *J Natl Cancer Inst.* 1989 Sep 6;81(17):1307-12.
- [3] W. Chen et al, 'Ultrasound Imaging of Spinal Vertebrae to Study Scoliosis', *Open Journal of Acoustics*, Vol.2 No.3(2012), Article ID:22602, 9 pages.
- [4] W. Chen et al, 'Reliability of assessing the coronal curvature of children with scoliosis by using ultrasound images', *J. Child. Orthop*, Vol. 7, No. 6, pp. 521-529, Dec. 2013.
- [5] R. Zheng et al., 'Intra- and Inter-rater Reliability of Coronal Curvature Measurement for Adolescent Idiopathic Scoliosis Using Ultrasonic Imaging Method—A Pilot Study', *Spine Deform.*, Vol. 3, No. 2, pp. 151-158, Mar. 2015.
- [6] W. Jiang et al, 'A fast 3-D ultrasound projection imaging method for scoliosis assessment', *MBE 2019* Vol. 16, pp. 1067-1081, Jan. 2019.
- [7] J. E. Herzenberg et al, 'Cobb Angle Versus Spinous Process Angle in Adolescent Idiopathic Scoliosis. The Relationship of the Anterior and Posterior Deformities', *Spine*, Vol. 15, No. 9, pp. 874-879, Sep. 1990.
- [8] C. Xu and J. L. Prince, 'Snakes, shapes, and gradient vector flow', *IEEE Trans. Image Process.*, Vol. 7, No. 3, pp. 359-369, Mar. 1998.
- [9] J. Malek et al, 'Automated Breast Cancer Diagnosis Based on GVF-Snake Segmentation, Wavelet Features Extraction and Fuzzy Classification', *J. Signal Process. Syst.*, Vol. 55, No. 1, pp. 49-66, Apr. 2009.
- [10] F. Liu et al, 'Liver segmentation for CT images using GVF snake'. *Medical Physics*, Vol. 32, No. 12 pp. 3699 -3706, Nov. 2005.
- [11] M.Cvancarova, F.Albregtsen, K. Brabrand, and E. Samset, 'Segmentation of ultrasound images of liver tumors applying snake algorithms and GVF', *Int. Congr. Ser.*, Vol. 1281, pp. 218-223, May 2005.
- [12] M. Kass et al, 'Snakes: Active contour models', *Int. J. Comput. Vis.*, Vol. 1, No. 4, pp. 321-331, Jan. 1988.
- [13] N. Otsu, 'A Threshold Selection Method from Gray-Level Histograms', *IEEE Trans. Syst. Man Cybern.*, Vol. 9, No. 1, pp. 62-66, Jan. 1979.
- [14] T. Y. Zhang and C. Y. Suen, 'A fast parallel algorithm for thinning digital patterns', *Commun. ACM*, Vol. 27, No. 3, pp. 236-239, Mar. 1984.
- [15] W. Jiang et al, 'A fast 3-D ultrasound projection imaging method for scoliosis assessment', *MBE 2019* Vol 16 Pages 1067-1081, Jan. 2019.
- [16] Cobb J. Outline for the study of scoliosis. *AAOS Instr Course Lect* 1948; 5:261-75.